

Jet impingement heat transfer effect on SCRAP

David McDougall¹, Theo von Backström², Matti Lubkoll³, and Ben Sebitosi⁴

¹ Solar Thermal Energy Research Group, Department of Mechanical and Mechatronic Engineering, Stellenbosch University, Cnr Banghoek Road & Joubert Street, Stellenbosch, South Africa; E-mail: 16801016@sun.ac.za

² Stellenbosch University; E-mail: twvb@sun.ac.za

³ Stellenbosch University; E-mail: matti@sun.ac.za

⁴ Stellenbosch University; E-mail: sebitosi@sun.ac.za

Abstract

The Spiky Central Receiver Air Pre-heater (SCRAP) receiver shows good potential as a pressurised air receiver for a combined cycle (CC). The spike tip is exposed to the highest solar flux which at the same time benefits from high cooling through the impinging jet of cold air. This study focusses on the development and validation of a numerical model that was further to be used to do an initial analysis on the effect of design parameters that can improve the performance.

The numerical model is developed and validated using experimental data. This preliminary analysis on the effect of altering different parameters shows that the parameter that has the biggest effect is the nozzle diameter. Reducing nozzle diameters induces excessive pressure drops to the system while increasing the thermal efficiency. A compromise is made between pressure drop and radiation losses to determine an initial estimation of an improved nozzle diameter of 15 mm, but there is more design improvement potential due to the effect of other geometric parameters. Therefore, an optimisation study is recommended.

Keywords: CSP, pressurised air receiver, SCRAP, impinging jet, jet impingement, CFD

1. Introduction

Concentrating solar power (CSP) has in the past 10-15 years grown significantly [1]. With the need for a transition to a more sustainable energy sector worldwide, renewable energy is getting more attention and CSP is being noticed for its ability to offer a more cost-effective means of storing energy than other renewable energy technologies. For CSP to be a competitive technology that adds value to the energy sector, it needs to be both dispatchable and cost effective.

Parabolic trough plants are relatively mature technology compared to central receiver plants. Central receiver plants are becoming the preferred technology because of their better efficiency and consequent reduced levelised cost of electricity

(LCOE). There is also research being done on using air as the heat transfer fluid and working fluid in open cycle gas turbines (OCGT) and combined cycles (CC).

The Stellenbosch University Solar Power Thermodynamic (SUNSPOT) cycle [2] is a CC concept (see Fig. 1) that utilises a CSP receiver that preheats the air before combustion to reduce fuel consumption. It also makes use of thermal storage to feed the Rankine cycle when the gas turbine is not running. This CC concept can have various configurations for various research purposes. In this study, the configuration includes a closed volumetric pressurised air receiver to preheat the air between the compressor and turbine of the gas turbine.

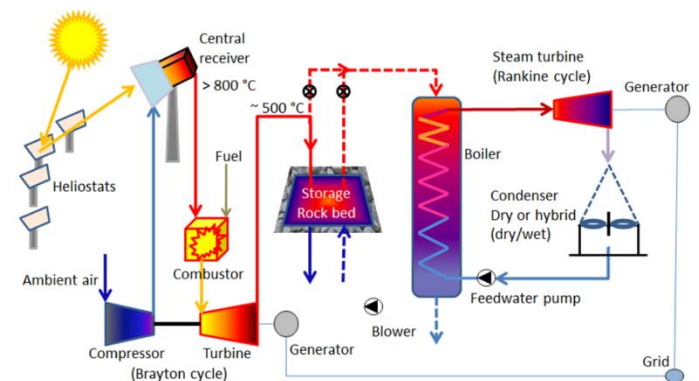


Fig. 1. Schematic diagram of the SUNSPOT cycle [2]

The purpose of the study is to determine what improvements can be made to the design of the Spiky Central Receiver Air Pre-heater (SCRAP) that was proposed by [3] and later, a performance analysis was done by [4]. One of the recommendations for further work was that the heat transfer characteristics at the spike tip be studied further in detail.

The receiver (SCRAP) is classified as a closed volumetric pressurised air receiver. It gets its name from its spiky appearance shown in Fig. 2. Each spike consists of two concentric tubes with the inner tube receiving pressurised air from the compressor and the outer annulus (with rectangular ducts) channelling the flow back to the combustion chamber.

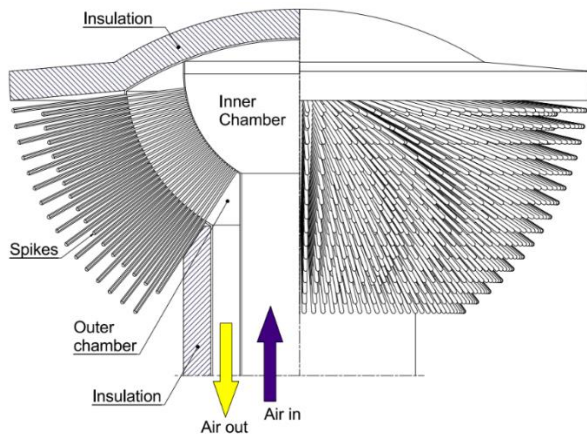


Fig. 2. SCRAP receiver with the left side sectioned [4]

Each spike is exposed to concentrated solar irradiation from a field of heliostats. The flow turns around in the end cap at the tip of each spike. The spike tip experiences the highest levels of irradiance and is therefore vulnerable to reaching elevated temperatures resulting in radiation losses and receiver material limitations.

The air exiting the inner tube impinges on the end cap or spike tip when it turns around to enter into the finned outer tube. This jet impingement can produce good heat transfer characteristics, increasing the air outlet temperature and reducing the radiation losses by reducing the spike tip surface temperature.

Fig. 3 shows the spike surface temperatures along the length as well as the air temperature from inlet to outlet of an improved design with a 7 mm nozzle diameter proposed by [4]. The spike used in Fig. 3 is a 1.3m spike that takes air from the compressor at 300 °C.

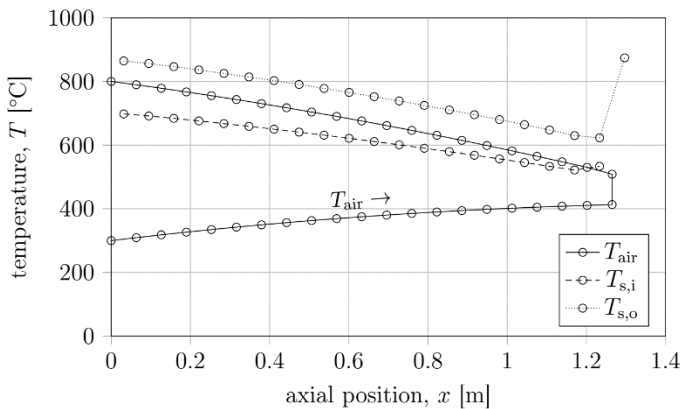


Fig. 3. Temperature profile of proposed improved design showing the air temperature, T_{air} , the inner tube surface temperature, $T_{s,i}$, and the outer tube surface temperature, $T_{s,o}$. [4]

The SCRAP receiver spike tip experiences maximum concentrated solar radiation (1.27 MW/m^2) in the centre of the end cap and this flux decreases parabolically towards the outer

tube surface (60 kW/m^2) according to the ray-tracing done by [4]. The concentrated flux can cause a hot spot on the centre of the end cap, limiting choice of materials for the receiver and causing excess radiation losses. The nature of jet impingement is such that the jet causes high Nusselt numbers at the stagnation point. This is desirable for the removal of heat at the centre of the end cap where the flux is high.

The jet impinges at the centre of the end cap of the spike as seen in Fig. 4. This is desirable because the solar flux is maximum at this point and the jet impingement produces maximum heat transfer at this point.

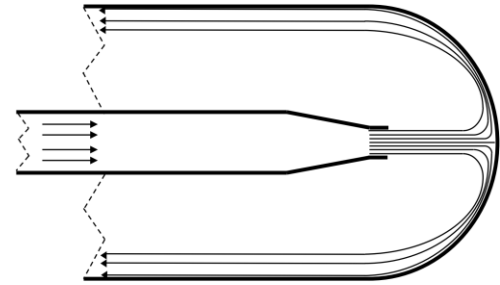


Fig. 4. Schematic showing the jet of air impinging on the spike tip

Although adding a nozzle at the end of the inner tube increases the heat transfer to the air and reduces the radiation losses, the nozzle can introduce undesirable pressure drops which directly affect the turbine efficiency by reducing the pressure ratio. Therefore, a balance between pressure drop and heat transfer is required to achieve the least performance losses and hence an increase system efficiency.

This study specifically looks at the heat transfer characteristics and pressure drop resulting from the introduction of a nozzle to the spike tip. The analysis presented in this paper includes developing and validating a numerical model that can be used to perform a parametric study on the tip heat transfer and flow conditions to study the effects of different parameters and ultimately propose flow and geometric alterations to improve the system performance of a gas turbine with SCRAP.

2. Literature review

It is known that jet impingement produces some of the best heat transfer characteristics of any heat transfer mechanism [5] which was one of Kröger's motivations for the SCRAP receiver's design. Studying literature reveals several effects and phenomena of the cooling mechanism such as nozzle diameter, nozzle-to-surface distance, Reynolds number, impingement surface geometry and the second peak phenomenon.

2.1. Reynolds numbers and typical Nusselt numbers

Jet impingement Reynolds numbers Re and Nusselt numbers Nu are calculated based on the nozzle diameter d . Smooth pipe flow is considered turbulent at $Re \geq 2300$ (see [6] and [7]). [8] states that free jets are considered turbulent at $Re \geq 100$ because of the entrainment of the surrounding fluid. The jet Reynolds numbers studied in this analysis are above 40 000. Therefore, all the flow cases are considered turbulent.

To characterise heat transfer between a fluid and a solid, the non-dimensional Nusselt number is often used. $Nu = hd/k$ where h is the heat transfer coefficient, d is the nozzle diameter, and k is the thermal conductivity of the fluid. Nusselt numbers from 50 to 200 are typically observed for impinging jet heat transfer [9].

Re is increased by either increasing the mass flow rate of the fluid or decreasing the nozzle diameter. The Nusselt number is typically directly proportional to the Reynolds number, Prandtl number and the nozzle-to-surface distance ratio L/d . The equation

$$Nu = CRe^n Pr^m f(L/d)$$

from [9] shows this relationship where C , m and n are constants.

2.2. Nozzle geometry

The smaller the nozzle, the higher the average heat transfer coefficient on the spike tip, but with a decreased nozzle diameter comes an increase in pressure drop. A compromise between radiation losses and pressure drop must therefore be made to find the combination that results in the highest system efficiency.

The shape of a nozzle significantly influences its pressure drop. The VDI atlas [8] encourages the use of a sloped ($\leq 20^\circ$) nozzle inlet to reduce the nozzle pressure drop. [10] found that simply introducing a 30° chamfer to the nozzle inlet increases the ratio of heat transfer coefficient and pressure drop by up to 30.8 %.

2.3. Nozzle-to-surface distance

The case study by [11] shows that the stagnation point Nusselt numbers reach a maximum at nozzle-to-surface distance ratios L/d of about 6 or 7. This is also observed by [12], [13] and [14].

It is, however, important to note that, in the context of SCRAP, the entire spike tip hemisphere should be cooled and not just around the stagnation point. The average surface temperature of the end cap is of interest. Reducing this reduces radiation losses.

2.4. Impingement surface geometry

Most literature on jet impingement involves a flat impingement surface. Implementing a concave curvature to the impingement surface can, according to [15], increase the heat transfer rates by up to 20 %.

The impingement surface being analysed in this paper is a concave hemispherical surface. An experimental study by [11] is introduced in more detail later. They find that an increased surface curvature causes an increase in heat transfer because the flow is increasingly forced against the surface.

A concave trough surface with a slot jet was studied by [16] and it was found that there is an optimal curvature intensity d/D around which the heat transfer characteristics decrease. The curvature intensity d/D is evidently directly proportional to the nozzle diameter d . [17] states that the curvature effect is accentuated by increasing Reynolds numbers.

2.5. Second peak phenomenon

Jet impingement heat transfer is typically known to have complex flow phenomena. The maximum Nusselt number is typically observed at the stagnation point, but it is often observed that another local maximum occurs. This is often referred to as the second peak phenomenon.

There have been several explanations for the phenomenon from literature over the years. An early observation (1965) by [18] is that the boundary layer formed from the stagnation point is thinned again when the jet's edges change direction as it hits the surface, speeding up the flow significantly. They claim that the thinning of the boundary layer and speeding up of the flow causes the second peak.

[19] and [14] state that the second peak is due to the entrainment at the edges of the jet that forms vortices that cause the secondary peak. [20] concludes that the second peak is merely accentuated by the fact that recirculated heated fluid causes a local minimum and hence creating the illusion of a second peak.

Later, [21] performed LES simulations and concluded that the second peak phenomenon is due to the combination of the recirculation of heated fluid, large eddies at the edges of the jet, as well as the speeding up of the fluid causing thinning of the thermal boundary layer. They further concluded that the second peak typically occurs between 1.4 and 2.8 nozzle diameters from the stagnation point.

2.6. Conclusion

The trends seen in literature on impinging jets are helpful when deciding what parameters to study in a sensitivity analysis. It is clear the Reynolds number Re , nozzle-to-surface ratio L/d , curvature intensity d/D and nozzle shape all affect the heat transfer capabilities of a jet. These parameters will be studied by analysing their sensitivity in the context of the spike tip of the SCRAP receiver.

3. Numerical model validation

A numerical model must be validated experimentally or analytically. An experimental study was done by [11] on the heat transfer capabilities of an impinging jet on a concave hemispherical impingement surface. They used an insulated concave hemisphere with diameter 381 mm and applied a uniform flux to the inner surface with gold film strips with current flowing through them. The layer of thermochromic liquid crystals allowed them to quantify the local surface temperatures when a fully developed jet impinges on the surface as shown in Fig. 5.

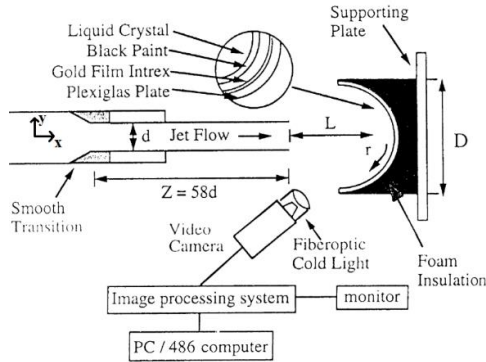


Fig. 5. Schematic of the experimental setup by [11]

The Nusselt number distributions along the concave surface in the radial direction were determined by [11] for 45 different parametric cases, including the combinations of: 3 Reynolds numbers Re (11 000, 23 000 and 50 000); 3 nozzle diameters (13, 21.5 and 34 mm); and 5 ratios (L/d) of nozzle-to-surface distance L to nozzle diameter d (2, 4, 6, 8 and 10).

The flow conditions and geometries recommended by [4] are Reynolds numbers Re (based on the nozzle diameter) ranging from 50 000 to 150 000, and nozzle diameters d of 5 mm to 20 mm where the hemisphere diameter D is 66 mm. This means that the parameters in the validation case study by [11] and the application to SCRAP overlap slightly, but for most cases, applying the validated model to SCRAP is an extrapolation from the experimental results.

To develop the validated model, the geometric and flow characteristics were replicated in ANSYS FLUENT™ assuming negligible turbulence in the azimuthal direction (about the axis) and hence reducing the problem to a 2D axisymmetric mesh to save computational time. The assumption of negligible turbulence in the azimuthal direction is because, at the Reynolds numbers being studied, the momentum in the radial and axial directions greatly outweighs the momentum in the azimuthal direction.

A very coarse depiction of the applied mesh to duplicate the experimental case can be seen in Fig. 6 with cell growth from the

hemisphere surface and inlet pipe (nozzle). A constant velocity inlet boundary condition is applied, and the inlet pipe is modelled as the same length as that used in the experiments ($58 \times d$) to allow the flow to develop fully. A 0 Pa pressure outlet is applied. The outlet region is studied at several outlet lengths and it is concluded that it does not affect the jet impingement flow, and therefore a small outlet region is modelled.

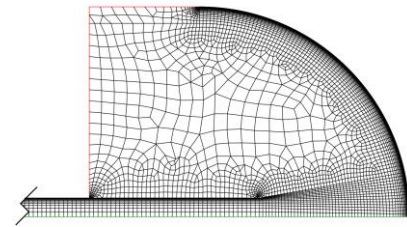


Fig. 6. Coarse 2D axisymmetric mesh

The convergence criterion selected for this analysis was $1e-6$ for all residuals except for the energy equation, which is $1e-12$. [22], amongst others, states that the mesh layers near the impingement surface should be very refined ($y^+ \leq 1$) so that the mesh can capture the boundary layer effects. The mesh should therefore be refined enough to achieve such y^+ values on this surface, as well as achieving convergence of the results with increasing cell counts. The mesh independence results are shown in Fig. 7 where the mesh with 145 800 cells was selected. This was performed on a case with a Re of 50 000 and the smallest nozzle diameter of 13 mm (maximum flow velocities) and therefore the mesh, when applied to other geometries and Re , will be sufficient because the maximum velocities produce maximum y^+ values and the wall cell growth is kept constant.

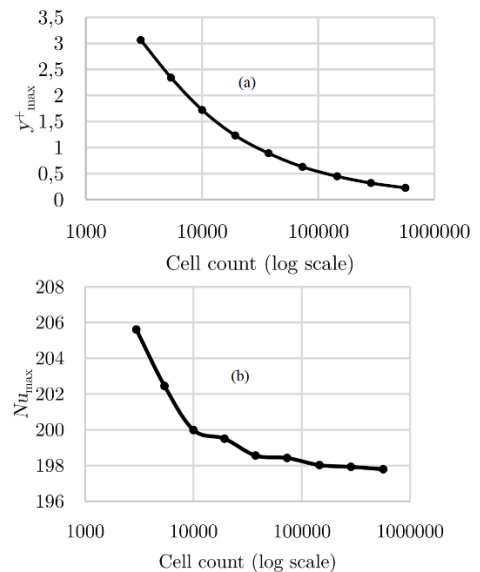


Fig. 7. Graphs showing the mesh dependence on grid refinement where (a) shows the maximum y^+ on the hemisphere wall and (b) shows the convergence of the maximum Nusselt number on this surface

In terms of Reynolds-averaged Navier-Stokes (RANS) models, [9], [23] and [24] show that the $k-\omega$ SST model produces good results for modelling impinging jet heat transfer with the capability of modelling the second peak phenomenon. To validate this, several models were used to obtain Nusselt number distributions for a case with Re of 50 000. The results shown in Fig. 8 show that the $k-\omega$ SST model produces the best correlation with the experimental results of [11]. In addition to the models included in Fig. 8, the $k-\epsilon$ standard model without enhanced wall treatment (EWT); the $k-\epsilon$ realizable model; the Spalart-Allmaras model; and the Reynolds stress model (with and without EWT) were analysed, but they all produced results outside of the scale of the plot and were hence excluded from the plot.

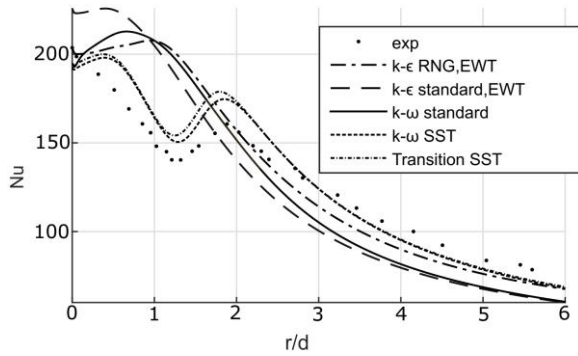


Fig. 8. Graph of Nusselt number on the concave surface for different numerical models

Once it was decided that the $k-\omega$ SST model is the preferred numerical model, all 45 cases were simulated with different settings to determine the best setup and the capabilities of FLUENT™ for jet impingement on a concave hemisphere.

The cases that are relevant to developing a model that is valid for SCRAP are the cases with similar flow and geometric characteristics to SCRAP. These cases are the cases with Re of 50 000 and nozzle-hemisphere diameter ratio d/D of 0.0892. Fig. 9 shows a comparison with the developed model and the experimental results for 2 different nozzle-to-surface distances.

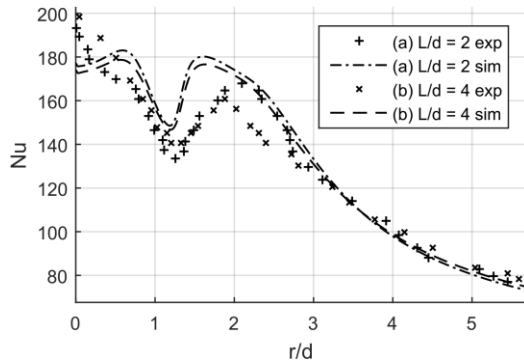


Fig. 9. Nusselt number distribution for two of the most relevant cases with $Re = 50\,000$, $d/D = 0.0892$, $L/d = 2$ for (a) and $L/d = 4$ for (b)

Since [11] did not publish the results for $L/d = 6$ and 8, the correlation is only conducted on $L/d = 2, 4$ and 10. The area-weighted averages of the Nusselt number distributions are compared. The developed model predicts the averages with a deviation of $\leq 8\%$ for $Re = 50\,000$; $d/D = 0.0892$ and 0.0564; and the above-mentioned nozzle-to-surface distances of $L/d = 2, 4$ and 10. The deviation is shown in Fig. 10.

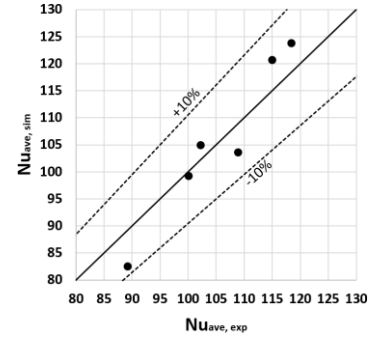


Fig. 10. Deviation of the area-weighted averages of the Nusselt number distributions simulated from the experimental results

In the overall performance analyses of the receiver performed by [4], the spike tip heat transfer was modelled using the $k-\epsilon$ standard model with various inlet pipe diameters providing a fully developed jet. This was done as a high-level determination of the heat transfer coefficients h for different nozzle diameters that was later used in his numerical model of the entire receiver. These simulations were replicated using the author’s validated model.

Good correlation with the heat transfer coefficients of [4] is achieved as seen in Table 1. There is, however, a noticeable deviation at a nozzle diameter of 26 mm which is not of interest to the author as will be seen later in the sensitivity analysis. The analysis performed by [4] slightly over-predicts the heat transfer coefficients.

Diameter [mm]	h [W/m ² K]	h from [4] [W/m ² K]	Deviation [%]
5	1556,2	1642	5,23
7	1321,4	1377	4,04
10	1035,8	1059,43	2,23
18	549,2	613	10,41
26	317	577	45,06

Table 1. A comparison of the heat transfer coefficients h of the developed model and the results of [4]

Since the developed model produces results within 10% of the experimental case study, it is determined that the model is accurate enough for the purposes of this study. The validated numerical model used for further investigation into the effects of the jet impingement heat transfer on the spike tip of the SCRAP receiver. A more detailed paper on the validation process is intended to be written in the future.

4. SCRAP nozzle geometric limitations

Fig. 11 shows the flow of air through a single spike. The nozzle for jet impingement is placed at the outlet of the inner tube causing a high-velocity jet to impinge on the hemispherical end cap. For the purposes of this analysis, the area weighted average of the heat transfer coefficient is used for comparison.

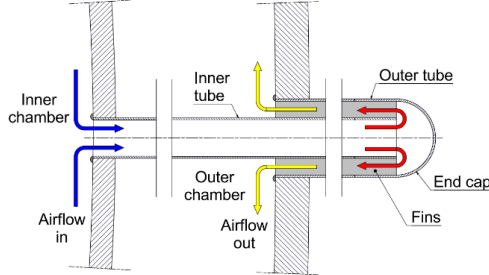


Fig. 11. Flow schematic of a single sectioned spike [4]

The flow characteristics are used from the recommended improved design by [4] in the sensitivity analysis. The following parameters are studied in this analysis:

- Nozzle diameter and hence Reynolds number (constant inlet flow rate)
- Nozzle-to-surface distance ratio L/d
- Nozzle inlet slope angle

Only the spike tip is modelled as a 2D axisymmetric geometry. The rectangular ducts in the outer tube are therefore not modelled. The inlet mass flow rate is 0.0326 kg/m^3 at a temperature of 700 K . A uniform flux is only applied to the end cap and nowhere else. This same flux as used in the numerical model by [4] is applied here as a constant over the surface of $463\,373.5 \text{ W/m}^2$. This is the area-weighted average of the assumed parabolic distribution.

The heat transfer effects as well as the pressure drop effects of the various parameters are analysed.

4.1. Nozzle diameter

The inner diameter of the inner tube is 26 mm and the inner diameter of the outer tube and hemisphere is 66 mm . Without a nozzle, the curvature intensity d/D is 0.39 . By attaching a nozzle to the end of the inner tube, it is expected that the pressure drop as well as the heat transfer will increase, while the end cap surface temperature will decrease.

Increased heat transfer results in decreased average surface temperature $T_{s,o}$ which henceforth decreases radiation losses Q_{rad} , where

$$Q_{rad} = \sigma \varepsilon A (T_{s,o}^4 - T_{sky}^4)$$

The pressure drop is taken from before the nozzle to the inlet of the outer annulus. Fig. 12 shows the results of the pressure drop and radiation losses for 6 different nozzle diameters. The nozzles all have an inlet slope angle of 30° .

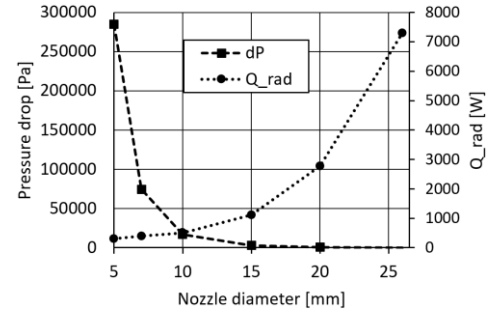


Fig. 12. Pressure drop (dP) and radiation losses (Q_{rad}) for different nozzle diameters

Pressure drop drastically increases with decreasing nozzle diameters, while the small nozzles, producing high heat transfer coefficients, result in low radiation losses. These two parameters have contradicting overall efficiency trends and a trade-off should therefore be made.

4.2. Nozzle-to-surface distance ratio L/d

Literature shows that the distance ratio L/d should produce a maximum stagnation point Nusselt number at about $L/d = 7$. This is analysed for confined and unconfined flat plate jet impingement as well as unconfined concave surface jet impingement.

The geometry of SCRAP is such that a confined concave surface jet impingement flow is produced. The confinement induces a large eddy and fluid that has already been heated is entrained into the edges of the jet. The entrainment of heated fluid reduces the heat transfer capabilities of the jet.

This large eddy effect increases as L/d increases and it is seen in Fig. 13 that as L/d increases (changing L while d is constant at 10 mm), the average surface heat transfer coefficient decreases. It is also seen that the pressure drop across the spike tip is at a minimum for $L/d = 4$.

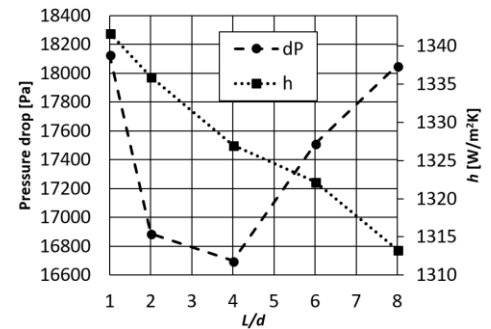


Fig. 13. Pressure drop (dP) and average heat transfer coefficient h of several nozzle-to-surface distances

4.3. Nozzle inlet slope angle

The expected effect of changing the nozzle inlet slope angle is that the pressure drop does not change and is at its minimum for angles less than 20° [25]. The analysis on a 5 mm nozzle with different inlet slope angles confirms this, as can be seen in Fig. 14.

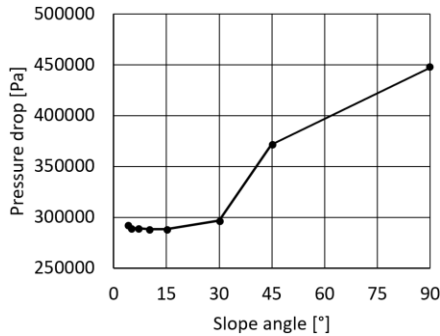


Fig. 14. Pressure drop for a 5 mm nozzle at different inlet slope angles (90° is a sharp entrance)

It is observed that the pressure drop is constant at its minimum for angles from 5° to 20° . Any sharper angles cause a drastic increase in pressure drop. The 4° slope also causes an increase in pressure drop that is assumed to be due to the extra length of pipe experiencing high velocities.

5. Results and discussion

In order to quantify the effect that the pressure drop and radiation losses have on overall system performance, they need to be quantified in an efficiency drop. From the sensitivity analysis, it is evident that the parameter that affects the performance most significantly is the nozzle diameter.

The radiation losses are quantifiable by converting them to a percentage of the input heat to get a percentage loss. The heat transfer rate reaching a spike of the receiver is 19 400 W. The percentage loss for the 10 mm nozzle from Fig. 12 is therefore 2.63 %.

To quantify a gas turbine's efficiency reduction due to a pressure drop between the compressor and the turbine, two references are cited. The performance characteristics of some *General Electric* turbines are published by [26], and it is stated that a pressure drop of 100 Pa results in an efficiency loss of 0.142 %. A second reference for this quantification by [27] shows that 100 Pa of pressure drop results in 0.12 % efficiency loss. The value of 0.142 % per 100 Pa published by [26] is used for this analysis. Since this quantification is specific to certain turbines and does not scale linearly, it is simply used in this study to identify the general effect of pressure drop.

To determine the compromise between pressure drop and heat transfer, their efficiency reductions are added together to obtain

a total efficiency drop. The optimal point is the minimum of this total. The pressure drops from the 5 mm and 7 mm nozzles are high and therefore are not covered in Fig. 15. Fig. 15 shows the total efficiency drop due to these two parameters and it is seen that, under these constraints, a 15 mm nozzle diameter would perform the best.

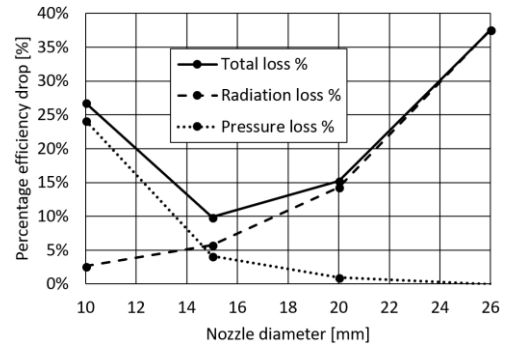


Fig. 15. Efficiency losses due to pressure drop and radiation for different nozzle diameters with a 30° inlet slope angle

The outlet temperature of the modelled spike tip is 790.35 K (a temperature rise of 90.35 K). This correlates well with [4]. This outlet temperature is not affected significantly by any of the geometric parameters, and hence the internal efficiency is not affected.

6. Conclusion

For the purposes of this study, the experimental case study by [11] is sufficient to validate the numerical model, but because the flow characteristics of SCRAP are extrapolated from the case study, a new experimental study on SCRAP would be advantageous.

It is found that there are several parameters and flow characteristics that affect the performance of the jet impingement heat transfer. The nozzle diameter affects the performance the most out of all the parameters. A trade-off is required between the pressure drop losses and radiation losses. A significant pressure drop is observed with nozzles with a smaller diameter than 10 mm. Combining the efficiency losses results in a preferred nozzle diameter of 15 mm.

Further work to reduce the pressure drop can be done by introducing more complex nozzle geometry. The current study assumes a constant heat flux on the spike tip, which is not accurate.

This preliminary parametric sensitivity study has given some insight into the relevant parameters, so that a full parametric study and a design optimisation are further recommended.

Acknowledgements

Partial funding for this work was provided by the National Research Foundation (NRF) of South Africa. The authors also thank the Centre for Renewable and Sustainable Energy Studies (CRSES) at Stellenbosch University for funding to attend the conference.

References

- [1] J. Sawin, K. Seyboth, and F. Sverrisson, "RENEWABLES 2017 GLOBAL STATUS REPORT," 2017.
- [2] D. G. Kröger, "SUNSPOT - The Stellenbosch UNiversity Solar POWER Thermodynamic cycle," Stellenbosch, 2012.
- [3] D. G. Kröger, "Spiky Central Receiver Air Pre-heater (SCRAP)," Technical report, Stellenbosch, 2008.
- [4] M. Lubkoll, "Performance Characteristics of the Spiky Central Receiver Air Pre-heater (SCRAP)," Doctoral Thesis, Stellenbosch University, 2017.
- [5] D. Cooper, D. C. Jackson, B. E. Launder, and G. X. Liao, "Impinging jet studies for turbulence model assessment-I. Flow-field experiments," *Int. J. Heat Mass Transf.*, vol. 36, no. 10, pp. 2675–2684, 1993.
- [6] H. Faisst and B. Eckhardt, "Sensitive dependence on initial conditions in transition to turbulence in pipe flow," *J. Fluid Mech.*, vol. 504, no. 1, pp. 343–352, 2004.
- [7] R. R. Kerswell, "Recent progress in understanding the transition to turbulence in a pipe," *Nonlinearity*, vol. 18, no. 1, pp. R17–R44, 2005.
- [8] W. Kast, *VDI Atlas Chapter L - Fluid Dynamics and Pressure Drop*, 2nd ed. Karlsruhe: VDI-Verlag GmbH, 2010.
- [9] N. Zuckerman and N. Lior, *Jet impingement heat transfer: Physics, correlations, and numerical modeling*, vol. 39, no. C. Elsevier Masson SAS, 2006.
- [10] L. A. Brignoni and S. V. Garimella, "Effects of nozzle-inlet chamfering on pressure drop and heat transfer in confined air jet impingement," *Int. J. Heat Mass Transf.*, vol. 43, pp. 1133–1139, 2000.
- [11] D. H. Lee, Y. S. Chung, and S. Y. Won, "The effect of concave surface curvature on heat transfer from a fully developed round impinging jet," *Int. J. Heat Mass Transf.*, vol. 42, pp. 2489–2497, 1999.
- [12] D. H. Lee, Y. S. Chung, and D. S. Kim, "Turbulent flow and heat transfer measurements on a curved surface with a fully developed round impinging jet," *Int. J. Heat Fluid Flow*, vol. 18, no. 1, pp. 160–169, 1997.
- [13] D. H. Lee, J. Song, and M. C. Jo, "The Effects of Nozzle Diameter on Impinging Jet Heat Transfer and Fluid Flow," *J. Heat Transfer*, vol. 126, no. August, pp. 554–557, 2004.
- [14] K. Kataoka, M. Suguro, H. Degawa, K. Maruo, and I. Mihata, "The effect of surface renewal due to large-scale eddies on jet impingement heat transfer," *Int. J. Heat Mass Transf.*, vol. 30, no. 3, pp. 559–567, 1987.
- [15] M. Sharif and K. Mothe, "Parametric study of turbulent slot-jet impingement heat transfer from concave cylindrical surfaces," *Int. J. Therm. Sci.*, vol. 49, no. 1, pp. 428–442, 2010.
- [16] E. Öztekin, O. Aydin, and M. Avci, "Heat transfer in a turbulent slot jet flow impinging on concave surfaces," *Int. J. Heat Mass Transf.*, vol. 44, no. 1, pp. 77–82, 2013.
- [17] G. Yang, M. Choi, and J. S. Lee, "An experimental study of slot jet impingement cooling on concave surface effects of nozzle configuration and curvature," *Int. J. Heat Mass Transf.*, vol. 42, pp. 2199–2209, 1999.
- [18] R. Gardon and C. Akfirat, "The role of turbulence in determining the heat-transfer characteristics of impinging jets," *Int. J. Heat Mass Transf.*, vol. 8, no. 1, pp. 1261–1272, 1965.
- [19] M. D. Fox, M. Kurosaka, L. Hedges, and K. Hirano, "The influence of vortical structures on the thermal fields of jets," *J. Fluid Mech.*, vol. 255, pp. 447–472, 1993.
- [20] M. Hadziabdic and K. Hanjalic, "Vortical structures and heat transfer in a round impinging jet," *J. Fluid Mech.*, vol. 596, pp. 221–260, 2008.
- [21] N. Uddin, S. O. Neumann, and B. Weigand, "LES simulations of an impinging jet: On the origin of the second peak in the Nusselt number distribution," *Int. J. Heat Mass Transf.*, vol. 57, pp. 356–368, 2013.
- [22] K. Heyerichs and A. Pollard, "Heat transfer in separated and impinging turbulent flows," *Int. J. Heat Mass Transf.*, vol. 39, no. 12, pp. 2385–2400, 1996.
- [23] B. Rama Kumar and B. Prasad, "Computational flow and heat transfer of a row of circular jets impinging on a concave surface," *Heat Mass Transf.*, vol. 44, pp. 667–678, 2008.
- [24] O. Caggese, G. Gnaegi, G. Hannema, A. Terzis, and P. Ott, "Experimental and numerical investigation of a fully confined impingement round jet," *Int. J. Heat Mass Transf.*, vol. 65, pp. 873–882, 2013.
- [25] W. Schabel and H. Martin, "Impinging Jet Flow Heat Transfer," in *VDI Heat Atlas*, 2nd ed., P. Stephan, Ed. Karlsruhe: VDI-Verlag GmbH, 2010, pp. 745–751.
- [26] F. J. Brooks, "GE Gas Turbine Performance Characteristics," Schenectady, 2005.
- [27] M. Mangel and H. Messe, "Efficient gas turbines by air cooling and pressure drop optimization," Mannheim, Germany, 2013.